Title
Wall stresses of early remodeled pulmonary autografts

Journal
Journal of Thoracic and Cardiovascular Surgery, 164(6)

ISSN
0022-5223

Authors
Xuan, Yue
Alonso, Edgardo
Emmott, Alexander
et al.

Publication Date
2022-12-01

DOI
10.1016/j.jtcvs.2021.08.058

Peer reviewed

HHS Public Access

Author manuscript

J Thorac Cardiovasc Surg. Author manuscript; available in PMC 2022 December 01.

Published in final edited form as:

J Thorac Cardiovasc Surg. 2022 December ; 164(6): 1728–1738.e2. doi:10.1016/j.jtcvs.2021.08.058.

Wall Stresses of Early Remodeled Pulmonary Autografts

Yue Xuan, PhD[1,*], **Edgardo Alonso, BS**[1,*], **Alexander Emmott, PhD**[2], **Zhongjie Wang, PhD**[1], **Shalni Kumar, BS**[1], **Francois-Pierre Mongeon, MD**[3], **Richard L. Leask, PhD**[2], **Ismail El-Hamamsy, MD**[4], **Liang Ge, PhD**[1], **Elaine E. Tseng, MD**[1]

[1]Division of Cardiothoracic Surgery, Department of Surgery, University of California San Francisco Medical Center and San Francisco VA Medical Center, San Francisco, CA

[2]Department of Chemical Engineering, McGill University, Montreal, Canada

[3]Division of Cardiology, Department of Medicine, Montreal Heart Institute, Montreal, Canada

[4]Department of Cardiovascular Surgery, Icahn School of Medicine at Mount Sinai, New York, NY

Abstract

Objective: Ross procedure is an excellent option for children or young adults who need aortic valve replacement because it can restore survival to normal aged-matched population. However, autograft remodeling can lead to aneurysmal formation and reoperation, and the biomechanics of this process is unknown. This study investigated postoperative autograft remodeling after Ross procedure by examining patient-specific autograft wall stresses.

Methods: Ross procedure patients who had intraoperative pulmonary root and aortic specimens collected were recruited. Patient-specific models (n=16) were developed using patient-specific material property and their corresponding geometry from cine magnetic resonance imaging (MRI) at one-year follow-up. Autograft ± Dacron for aneurysm repair and ascending aortic geometries were reconstructed to develop patient-specific finite element models, which incorporated material properties and wall thickness experimentally measured from biaxial stretching. Multiplicative approach was used to account for pre-stress geometry from *in-vivo* MRI. Pressure loading to systemic pressure (120/80) was performed using LS-DYNA software.

Results: At systole, first principal stresses were 809kPa (25-75% IQR, 691-1219kPa), 567kPa (485-675kPa), 637kPa (555-755kPa), and 382kPa (334-413kPa) at autograft sinotubular junction (STJ), sinuses, annulus, and ascending aorta, respectively. Second principal stresses were 360kPa (310-426kPa), 355kPa (320-394kPa), 272kPa (252-319kPa), and 184kPa (147-222kPa) at autograft STJ, sinuses, annulus, and ascending aorta, respectively. Mean autograft diameters were 29.9±2.7mm, 38.3±5.3mm, and 26.6±4.0mm at STJ, sinuses, and annulus, respectively.

Corresponding author: Elaine E. Tseng, MD, Division of Cardiothoracic Surgery, University of California San Francisco, San Francisco VA Medical Center, 500 Parnassus Ave. Suite 405W, San Francisco, CA 94143, Office: 415-221-4810 x23452, Fax: 415-750-2181, Elaine.Tseng@ucsf.edu.

*Authors contributed equally to the current work.

Presented at the American College of Surgeons Clinical Congress 2020 Scientific Forum, Exclusive Virtual Event, October 4-7, 2020

Conflicts of Interest: None applicable.

CHR approval number: 15-16989, 12-08529, 2021-2927

IRB waived the need for Written Informed Patient Consent for Publication

Conclusions: Peak first principal stresses were mainly located at STJ, particularly when Dacron reinforcement was used. Patient-specific simulations lay the foundation for predicting autograft dilatation in the future after understanding biomechanical behavior during long-term follow-up.

Keywords

Ross procedure; pulmonary autograft; remodeling; dilatation; computational modeling; wall stress; finite element analysis; Ross operation; heart valve replacement; autograft

Introduction

The Ross procedure has emerged as an ideal choice for surgical aortic valve replacement (SAVR) in pediatric patients and young adults[1, 2] who desire an active lifestyle, and prefer to avoid life-long anti-coagulation. Benefits of the Ross procedure also include excellent hemodynamics, and a living valve that can grow with children and young adults. More importantly, recent evidence suggests that the pulmonary autograft restores patient life-span to normal age-matched population-based survival[3–5]. Controversies regarding the Ross procedure remain including 1) converting a single to double valve operation, 2) increased technical complexity compared to mechanical or stented bioprosthetic valve replacement, 3) need for reoperation due to autograft dilatation with aneurysm formation or aortic insufficiency, and 4) need for reoperation for pulmonary homograft stenosis[6, 7]. Specialized centers[5, 8–11] with Ross expertise have largely overcome issues with the technical complexity of the operation, demonstrating excellent operative outcomes, while oversized pulmonary homografts have reduced concerns regarding homograft stenosis[12].

Pulmonary autograft dilatation remains the primary concern and can lead to reoperation due to aneurysm formation and/or autograft valve insufficiency, though reported reoperation rates vary among different institutions[2, 13, 14]. Ross techniques vary, including subcoronary[15, 16], full root with and without native aortic support[11, 17, 18], root inclusion[11], as well as differences in length of pulmonary artery utilized, and use of autograft annulus or sinotubular junction (STJ) reinforcement[19, 20]. While such technical differences have been cited as potential causes for differences in long-term reoperation rates[17], for the full root replacement technique. Fundamentally, the autograft root is transposed from the low-pressure pulmonary environment to the high-pressure systemic one. Normally, the pulmonary root experiences a mean arterial pressure (MAP) of ~15mmHg in adult pulmonary circulation, while MAP in systemic circulation is ~93mmHg, a greater than 6x pressure change for the autograft immediately after transposition. Previously, we demonstrated in a single human autograft finite element (FE) model that wall stresses on the autograft root increased dramatically upon immediate exposure to systemic pressure without concurrent dilatation[21]. These wall stress changes may trigger and influence autograft remodeling including increased wall thickness and compliance; changes we have shown evident in late failed aneurysmal autografts 13 years after initial Ross operation[22]. However, not all autografts dilate; therefore, determining the degree of increased autograft wall stresses after Ross procedure may aid understanding of the risk of long-term dilatation and aneurysm formation. Yet, the nature of postoperative autograft biomechanics in any given patient is unknown. Our objective in this hypothesis-generating study was to examine

patient-specific autograft wall stresses after Ross procedure using patient-specific imaging at one year postoperatively combined with corresponding material properties determined from intraoperative tissue specimens to initiate our longitudinal tracking in correlation with early remodeling. To our knowledge, this is the first work that presents patient-specific stress distribution using image-based geometry, experimentally measured material properties for each patient combined with the detailed surgery technique with and without Dacron replacement of the dilated ascending aorta. Since wall stress cannot be directly measured *in vivo*, we performed finite element analysis (FEA) using patient-specific geometry and material properties to determine autograft wall stresses.

Materials & Methods

Patients undergoing the Ross procedure were recruited consecutively at Montreal Heart Institute (MHI) (n=290) and the subset of patients with both follow-up 1-year magnetic resonance imaging (MRI) and intraoperative pulmonary root specimen collection for patient-specific material properties were included in the study (n=16). The study was approved by the institutional review board at MHI, San Francisco Veterans Affairs Medical Center (SFVAMC) and Committee on Human Research at University of California San Francisco (UCSF) and written informed consent was waived for publication. Pulmonary root samples for all patients (n=16) and ascending aortic samples for most patients (n=10) were excised intraoperatively via a standardized approach, performed by a single surgeon. Specimens for biaxial stretch testing were taken from the anterior quadrant 3mm distally above the respective commissures for pulmonary and aortic roots. Patients at the time of operation with enlarged ascending aortic diameters additionally underwent an interposition Dacron graft.[17] Extracted specimens underwent biaxial stretch testing up to 75% strain as previously described[23] to measure patient-specific material properties. The stress-strain data was then fitted to the fiber-embedded hyperelastic material model[24] to derive the patient-specific material property parameters (Supplemental Table 1). Sample thicknesses were measured. De-identified MRI images were transferred to SFVAMC for patient-specific FE modeling.

Development of patient-specific models

Patient-specific simulations integrated image-based geometry and experimental measurements of material properties for each patient. Also, fiber-embedded hyperelastic material model was used to represent the non-linear material property of aortic and pulmonary tissues. The material model was previously described[24] and the governing equation of the two groups of dispersed collagen fibers is listed below

$$\Psi_{collageni}(\mathrm{C}) = \frac{k_1}{2k_2}\left[\exp\left(k_2\bar{E}_i^2\right) - 1\right], i = 1, 2$$

where $\bar{E}_i$ is an invariant that reflects the impact of each fiber family deformation on strain energy function; k_1 an k_2 are material parameters determined by mechanical testing of the material. The patient-specific material properties were also averaged and utilized in a second set of pressure simulations for each patient model to compare the impact of patient-specific

material properties vs. the group averaged material properties on wall stress (Supplemental Table 1).

MRI images acquired 1-year postoperatively were then manually contoured under diastolic pressure to reconstruct 3D geometry of pulmonary autograft and distal ascending aorta. Images were exported as Digital Imaging and Communications in Medicine (DICOM) files and imported into MeVisLab (http://www.mevislab.de/home/about-mevislab) for image segmentation. Next, smooth three-dimensional surfaces with patient-specific thicknesses (Figure 1) were constructed and imported into TrueGrid (XYZ Scientific, Applications, Inc., Pleasant Hills, CA) to generate FE hexahedral meshes (Figure 1) which were subsequently imported into LS-DYNA (LSTC Inc., Livermore, CA) for physiological pressure simulations. Since *in vivo* images represented pre-stressed geometries under *in vivo* physiologic blood pressures, we used a modified update-Lagrangian method to account for pre-stress through an iterative process[24]. Distal ascending aorta (AscAo) and pulmonary autograft were modeled as incompressible hyperelastic material, comprised of extracellular matrix reinforced with dispersed collagen fibers[24]. As previously described, dynamic simulations were performed by applying physiologic systemic pressure loading conditions to inner lumens[21]. Physiologic cardiac cycle of 800ms duration was applied which included systole, increasing arterial pressure up over 300ms from diastolic (80mmHg) to peak systolic pressure (120mmHg), followed by 500ms of diastole, decreasing downwards to minimum diastolic pressure.

Data Analysis and Statistics

Simulation results were examined at times corresponding to peak systolic pressures to measure wall stress and autograft diameter. The 99th-percentile wall stress as previously described[25] was examined in this study, as it more reproducibly represents peak stress by avoiding the non-physiologic peak stresses that can occur from inhomogeneities in the FE mesh. References to peak wall stresses will hereafter be represented by 99th-percentile wall stresses. To measure maximum diameter, distances between the furthest sets of nodes on perpendicular planes to the centerline were tracked at each sub-region of the root and ascending aorta. The reproducibility of the current study was performed by having authors E.A. and Y.X. independently develop separate sets of computational models from the MRI images of each subject. Both performed independent FEA and stress distributions and magnitudes were compared. Validation of computational models was performed by comparing the model geometry against the MRI geometry.

Continuous measurements of autograft size and patient age are presented as mean±SD, while wall stresses are presented as median and (25%-75%) interquartile range. Categorical measurements are presented as numbers and percentages. The data were tested for normal distribution using the Shapiro-Wilk test. Spearman rank correlation coefficients were used for the correlation between autograft diameter and wall stress, and continuous and categorical variables were compared using Mann-Whitney U-test and Kruskal-Wallis test, respectively. A p-value <0.05 was considered statistically significant. Statistical analyses were performed using R (R 3.6 www.r-project.org).

Results

Table 2 identifies the clinical profiles of each Ross study patient. The study population was 63% male (n=10), 37% female (n=6), with a mean age of 47.8 ± 12.9, ranging 17-60 years old. Clinically, 81% (n=13) of the group had a bicuspid aortic valve and 19% (n=3) had a unicuspid aortic valve, with 56% (n=9) having aortic stenosis and the remainder having mixed stenosis and regurgitation. Average wall thickness of the pulmonary autografts and ascending aorta were 1.2 ± 0.2mm and 1.7 ± 0.3mm, respectively. Postoperative mean pulmonary autograft size was 3.8 ± 0.5cm, ranging 3.1-4.8cm. Postoperative maximum autograft diameters were significantly larger in men than women ($p<0.001$). Postoperative annulus diameters (2.7 ± 0.4cm) were significantly smaller than autograft STJ (3.0 ± 0.3cm, $p=0.03$), which were in turn smaller than sinuses (3.8 ± 0.5cm, $p<0.001$). Postoperative autograft sinus diameters were also significantly larger than those of annulus ($p<0.001$) as expected.

In comparing the 1yr postoperative pulmonary autograft diameters to the preoperative aortic diameters at each subregion (14 patients out of the 16), significant reduction of diameter was found at the annulus from 3.4 ± 0.7cm (preop aortic) to 2.7 ±0.4cm (postop autograft) ($p<0.001$) and STJ from 3.3 ± 0.7cm (preop aortic) to 3.0 ± 0.3cm (postop autograft) ($p=0.035$). The diameter at the ascending aorta was not significantly different from preoperatively 3.8 ± 0.6cm to postoperatively at 1-year, 3.6 ± 0.4 ($p=0.15$). No significant differences were found in the preoperative aortic sinus diameter 3.8 ± 0.7cm and the postoperative autograft sinus diameter 3.8 ± 0.5cm ($p = 0.42$) at 1-year.

Interestingly, the pulmonary autograft diameters did not change significantly at the annulus ($p=0.29$) from preoperative pulmonary pressures to postoperative aortic systemic pressures at 1-year (2.8 ± 0.7cm vs 2.7 ± 0.4cm, respectively, $p=0.29$). Similarly, the autograft diameters at the STJ also did not significantly change from the preoperative pulmonary pressures to the postoperative aortic systemic pressures at 1-year (2.9 ± 0.5cm vs 3.0 ± 0.3cm, respectively, $p=0.13$). On the other hand, the sinus diameters of the pulmonary autograft did increase in size from preoperative pulmonary position (2.8 ± 0.5cm) to postoperative aortic position at 1-year (3.8 ± 0.5cm), $p<0.001$.

At end systole, median first and second principal stresses on the pulmonary autograft overall, which roughly correlate with circumferential and longitudinal directions, were 651.1kPa (599.0-796.8kPa) and 345.2kPa (317.2-396.4kPa) ($p<0.001$) (Figure 2). Peak stresses in the autograft subregions: STJ, sinuses of Valsalva, and annulus were also examined. Peak first and second principal stresses at autograft STJ were 808.8kPa (691.2-1219.0 kPa) and 359.7kPa (310.1-426.3kPa), respectively ($p<0.001$). At autograft sinuses, peak first and second principal stresses were 566.7kPa (484.8-675.2kPa) and 355.5kPa (319.7-394.1kPa), respectively ($p<0.001$). At the annulus, peak first and second principal stresses were 636.8kPa (554.7-755.0kPa) and 271.9kPa (252.4-318.7kPa), respectively ($p<0.001$). Above the autograft and/or Dacron STJ reinforcement, peak first and second principal stresses on the AscAo were 381.5kPa (333.9-413.2kPa) and 183.9kPa (146.9-221.8kPa), respectively ($p<0.001$). Overall, peak wall stresses in the autograft as a

whole and in each subregion were significantly different between first and second principal stresses as related to circumferential and longitudinal directions.

When comparing among autograft subregions (Figure 3), peak first and second principal stresses were not significantly different between autograft STJ and annulus (p=0.08 and p=0.07, respectively). Peak first principal stresses in autograft sinuses were also not significantly different than that in the annulus (p=0.27), or STJ (p=0.05). In contrast, peak second principal stresses in autograft sinuses were significantly greater than that in the annulus (p=0.01), but were not significantly different than that in the STJ (p=0.95, Figure 3). Notably, peak first and second principal stresses of all autograft subregions were significantly greater than those of the distal AscAo (p<0.001).

Among the n=16 patients, n=11 had an ascending aortic repair with Dacron interposition, while n=5 did not. Peak first principal stresses were significantly greater in those with Dacron interposition grafts than those without at the STJ, 895(809-1280)kPa vs. 507(363-599)kPa, respectively (p=0.002), and at AscAo, 387(377-479)kPa vs. 274(274-309)kPa, respectively (p=0.02), but not in the sinuses, 592(511-828)kPa vs. 488(475-588)kPa, respectively (p=0.21), or at the annulus, 671(597-808)kPa vs. 565(479-600)kPa, respectively (p=0.05). Similarly, peak second principal stresses were significantly greater in patients who had Dacron interposition grafts than those without at the STJ, 403(360-512)kPa vs. 219(206-255)kPa, respectively (p=0.003), and at the AscAo, 201(184-240)kPa vs. 137(116-141)kPa, respectively (p=0.002), but not at the sinuses, 365(349-441)kPa vs. 321(315-334)kPa, respectively (p=0.14), nor at the annulus, 290(266-331)kPa vs. 241(212-264)kPa, respectively, (p=0.14).

When examining the relationship between peak autograft stresses and diameter, pockets of peak wall stresses occurred most often in the STJ region rather than the sinuses, which had the largest diameter (Figure 3). Correlation between maximum diameter and peak stresses was extremely weak along both the circumferential (r=−0.29) and longitudinal (r=−0.21) directions (Supplemental Figure 1). Autograft thickness was weakly related to the first principal stress (r=−0.48).

Lastly, we examined the influence of patient-specific vs averaged material properties on wall stresses, since clinical determination of patient-specific material properties will be time-consuming and potentially challenging for clinical application. Overall, there were no significant differences in the magnitude and location of first and second principal stresses when using patient-specific vs. averaged material properties. In each subregion, using patient-specific vs. averaged material properties revealed no significant differences in first principal wall stresses in STJ (p=0.90), sinuses (p=0.98), annulus (p=0.98), and ascending aorta (p=0.72); and similarly, no significant differences in second principal wall stresses in STJ (p=0.70), sinuses (p=0.98), annulus (p=0.40) and ascending aorta (p=0.55). Detailed wall stresses in each subregion are shown in Table 4.

The distensibility from diastole to systole was calculated at each subregion of the pulmonary autograft (Table 5). Without Dacron replacement of the ascending aorta, distensibility of STJ

was similar to the annulus. Distensibility of the sinus was generally less than at STJ and annulus.

Our computational models were validated by overlaying the geometry from MRI reconstructed images to geometry from our computational models at diastolic pressure (Supplemental Figure 2). The geometry from our diastolic simulations tightly overlapped with those from MRI. Furthermore, in the reproducibility study, stress distribution of each aortic model between the two independent investigators was nearly identical, and variation of peak stress magnitudes was <6% which was within the accepted range of prior interobserver study[26]. Figure 4 summarizes the overall study design and results.

Discussion

We studied the maximum diameters and patient-specific *in vivo* wall stresses of postoperative pulmonary autografts at 1-year after Ross operation. This study presents the most accurate patient-specific simulation by integrating image-based geometry, experimental measurements of material properties from intraoperative tissue for each patient, and the detailed surgery technique with and without Dacron replacement of the dilated ascending aorta. Peak first and second principal stresses were seen at autograft STJ and were primarily driven by the placement of Dacron interposition graft. Notably, in all autograft subregions, peak first and second principal stresses were significantly greater than those in the distal AscAo. These elevated wall stresses along the autograft may trigger continued remodeling over time and may be associated with later autograft dilatation. At this early time-frame, autograft dilatation was not seen despite elevated autograft wall stresses compared to lower wall stresses in corresponding native distal ascending aorta.

Understanding the magnitude and distribution of wall stress experienced by the pulmonary autograft as it moves from its low-pressure pulmonary circulation to systemic pressure fills a fundamental gap in knowledge to understand autograft remodeling. Autograft dilatation likely reflects the inability of the native pulmonary root to adapt to demands of the systemic circulation. Using computational modeling and FEA, we previously demonstrated in a single human autograft, a significant 6-fold increase in autograft wall stress when exposed to the higher MAP (~93mmHg) in systemic circulation, from the lower MAP (~15mmHg) of pulmonary circulation. However, this model did not incorporate patient-specific material properties, unlike our present study[21]. In this study, using patient-specific material properties and *in vivo* autograft geometries, autograft wall stresses at one-year post-Ross operation were still higher than their corresponding distal ascending aorta controls regions, but no significant autograft dilatation was seen. This can be explained by the nonlinearity of the autograft stress-strain curve, where at systemic pressure the increased stiffness of the autograft material properties prevents early dilatation.

Pulmonary Autograft Diameter

Our results showed that in early autograft remodeling one-year post-operatively, maximum diameter occurred as expected at the sinuses, while STJ and annulus were well constrained. Average sinus diameter was 29% larger than in the STJ (38.3mm vs. 29.8mm), and 44% larger than in the annulus (38.3mm vs. 26.6mm). Notably, compared to the preoperative

baseline aortic annulus and STJ diameters, the postoperative autograft reduced both the annulus and STJ diameters. However, the autograft preoperative diameters at pulmonary pressures did not significantly change from the autograft postoperative diameters at 1-year at the annulus and STJ. These findings suggest that the technique Dr. El-Hamamsy used to place the autograft annulus in the subannular position constrained the annulus diameter postoperatively, just as the Dacron interposition graft at the STJ constrained the STJ from dilating at systemic pressure. However, the sinuses of the autograft did dilate from preoperatively at pulmonary pressures to postoperatively at 1-year at systemic pressures. But, the diameter of the autograft sinuses did not significantly differ in size postoperatively from the aortic sinuses preoperatively at systemic pressure. This suggests that at systemic pressure the autograft achieved the size of the aortic sinuses which is larger than autograft sinuses at pulmonary pressures. It is reassuring that the autograft could achieve normal aortic sinus dimensions without dilatation. Clinical follow-up echocardiography of human pulmonary autografts after the Ross operation have shown sinus diameters of 36mm immediately following cardiopulmonary bypass by Hokken et al.[27] and 37.3mm by Carr-White et al.[28]. These results were well correlated to our sinus diameter of 38.3mm.

Clinically, STJ diameter was found to be an independent predictor of autograft regurgitation which led to reoperation[2]. Failed autografts showed STJ dilatation without associated sinus dilatation[2], though this was not uniformly so and sinus dilatation was also demonstrated. Progressive autograft enlargement was found pronounced at sinuses and STJ in 119 patients, whose mean sinus and STJ diameters increased from 30.8 to 42.4mm and 26.6 to 32.2mm, respectively, at 10 years[2]. David et al. showed dilated sinuses with STJ dilatation with the aortic root replacement technique[29]. Another group observed a trend of more marked STJ dilatation in serial follow-up over four years[28]. Overall, these clinical follow-up studies suggest that STJ remodeling to accustom the autograft to systemic pressure may be critical in discerning autografts at risk of dilatation vs not. In this study n=11 patients had Dacron interposition which constrained STJ from dilatation postoperatively.

Maximum Diameter and Peak stress

Interestingly, peak stresses were not located in the region of maximum diameter in the majority of our study population, suggesting that factors such as complex noncylindrical geometries contributed to the stress distribution, and were not well predicted by diameter using LaPlace’s Law. Our results showed peak stresses in the STJ despite the largest diameter occurring in the sinuses. Since n=11/16 patients had Dacron interposition, Dacron graft had particular impact on wall stresses. Dacron interposition technically reinforces the STJ similarly to felt strip reinforcement. Notably our results showed that this reinforcement had no impact on stresses in the sinuses or annulus. STJ stresses were significantly greater as expected due to the transition from native autograft tissue to a much thinner and stiffer Dacron material. One criticism of the Ross procedure is need for reoperation due to autograft dilatation and aneurysm formation because of concern for autograft dissection or rupture. Since dissection/rupture can be considered a mechanical failure when wall stress exceeds wall strength, autograft dilatation alone may not be an indication for reoperation if 1) the leaflets remain competent, and 2) autograft stresses do not exceed wall strength. Circumferential stresses account for autograft expansion, while longitudinal stresses control

elongation. While STJ circumferential stresses were largest, Dacron actively constrains the STJ diameter and also prevents dissection propagation. It is noted that the protective role of Dacron in this situation is similar to other Ross surgical techniques to stabilize the STJ such as STJ reinforcement with felt or full root inclusion as shown in previous studies[30–32]. These techniques were found to promote longer freedom from reintervention.

The underlying biomechanical mechanism is similar in each of those scenarios. STJ stabilization with Dacron interposition, felt reinforcement, or full inclusion root techniques physically confines the STJ from later expansion to prevent remodeling. Dacron or felt provides strong support as a loading bearing structure which releases the high stress concentration that may drive the autograft remodeling given the strength of the materials. Because the sinuses are spared of the increased stresses with these techniques, other non-inclusion root techniques may potentially be protective of dilatation, such as partial inclusion of the noncoronary sinus aortic wall to support the autograft sinuses, as long as the STJ remains stabilized by Dacron or felt. In our models, both autograft STJ and sinuses had stresses that were greater than that of their respective distal AscAo as well as those reported for normal human aortic sinuses (100-130kPa)[33]. Further follow-up over time of autograft stresses in these specific patients will be essential to understand if wall stresses diminish and approach normal aortic wall stresses over time. Understanding *in vivo* autograft sinus stresses will be important for correlation of future autograft dilatation.

This study is unique in that patient-specific material properties of pulmonary root and AscAo were available at the time of Ross operation to incorporate in the FE models along with *in vivo* MRI patient-specific 1-year post-operative Ross geometries to determine patient-specific wall stresses. As further understanding of Ross biomechanics is acquired during follow-up, the challenges in using biomechanics to predict adverse Ross remodeling and autograft dilatation will be to acquire patient-specific material properties *in vivo.* We have previously demonstrated the ability of displacement encoding with stimulated echo (DENSE)-MRI to determine patient-specific material properties in ascending thoracic aortic aneurysms[34]; however, our DENSE-MRI protocols at this time are vendor-specific and our Siemen's based sequences were not available for the retrospectively acquired MRI images from the Phillips scanners in Montreal. As such we limited the study to those patients whose actual tissue specimens were available for material property assessment experimentally and examined the influence on FEA derived stress results. We found no significant differences in wall stress magnitudes or distribution based upon patient-specific vs averaged material properties (Table 4). With hundreds of patients that received a 1-year postoperative MRI but did not have intraoperative specimen collected, these results suggest we can reasonably approximate patient-specific wall stresses with group-averaged material properties. This will aid in simplifying the computational modeling process and applying FEA more broadly to the majority of Ross patients with follow-up imaging.

We developed patient-specific Ross models to lay the foundation for understanding autograft remodeling over time. We hypothesize that higher autograft wall stresses drive autograft remodeling and that autograft dilatation results from abnormal remodeling responses such as increased autograft compliance as we previously found in failed autografts[22] or failure of autograft wall stresses to normalize towards aortic wall stresses. This initial study of

postoperative pulmonary autografts sets the stage to understand autograft wall stress changes over time in mid- and long-term follow-up with an expanded patient cohort. Patient-specific autograft simulations could fill the gap in knowledge of what leads to autograft dilatation. Using pre-operative MR imaging, virtual Ross simulations of stress profiles coupled with evaluation of changes in stress distribution and magnitude over time at 5-10 years could identify predictors for dilatation. Anticipating which patients are at risk of autograft dilatation and thus during Ross procedure require adjunctive preventative measures, such as Dacron inclusion root to support autograft sinuses, rather than proximal and distal support of non-inclusion root with STJ stabilization with Dacron/felt or annular support, would be extremely beneficial given the additional technical complexities. For postoperative patients, early Ross remodeling simulations could stratify patients at higher risk for dilatation and aneurysm formation based on their post-operative imaging and allow opportunity for earlier medical optimization such as stricter blood pressure control and more frequent follow-up.

Study Limitations

While the application of the Ross procedure is not widespread, we selected the patients with intraoperative tissue and postoperative MRIs, which further reduced the study cohort. Such highly selected cohort ensured us to develop the most accurate computational models based on patient-specific geometry and material properties in this preliminary study. With this cohort of patients, we were able to have a proof of concept, by identifying the extent wall stress plays in early remodeling and highlighting how averaged-material properties may provide comparable results. This will allow us to further expand future studies to additional patients over longer follow-up.

In our simulations, we focused on the effects of pressure loading on diameter and wall stress. As such, valve leaflets were not included in the models, since velocity distribution and flow characteristics using computational fluid dynamics or fluid shear stress using fluid-structure interaction were not examined.

Our goal was to create the best approximation of patient-specific models in the early post-operative period to establish a baseline for the remodeling process anticipated over the following 10-15 years. The material property was measured from extracted intra-operative specimen, however due to clinical limitations the earliest 3D imaging available is 1-year postoperatively. Our previous study of failed Ross autografts indicated that the time of the autograft in circulation prior to autograft dilatation and reoperation was 13 years[22]. While we have no information regarding the time course of material property change, it is reassuring that the autografts did not become aneurysmal at this time frame. These models were meant to reflect the postoperative baseline autograft stresses from which to compare future work with patient-specific follow-up at 5 and 10 years after the Ross procedure. This future follow-up will allow us to test the hypothesis that autograft biomechanical remodeling influences dilatation over time. Lastly, it is to be noted that patient-specific material properties of aortic and pulmonary tissue are variable as to be expected based on variations in age, sex, disease process, etc and as witnessed by surgeons in the operating room. Despite the variability in material parameters, we assessed the impact of averaged vs. patient-specific material properties in the simulation results and found no significant

differences. We plan to simplify future computational modeling processes for the vast majority of Ross patients based on these data.

Finally, we used normotensive blood pressure 120/80 for all patients to assess wall stress consistently within the group, but clinically, these patients were subjected individually to strict blood pressure control, often ≤100mmHg during the early remodeling period, to effectively reduce the peak autograft stresses.

Conclusions

Patient-specific modeling of pulmonary autograft after Ross procedure demonstrated greater *in-vivo* wall stresses at the sinotubular junction, sinuses, and annulus when compared to the internal controls of wall stresses in the native distal ascending aorta at 1 year post-operatively. Despite elevated autograft wall stresses, no autograft dilatation was seen at this early time frame, due to the stiffness of the autograft in that region of the stress-strain curve. Whether autograft wall stresses normalize to the magnitude of the native aorta over time will be important to determine in future studies. Dacron graft interposition anatomically constrained autograft dilatation at the STJ, and is associated with increased STJ stresses due to the Dacron material stiffness, but had little effect in the annulus and sinus regions. This study fills a critical knowledge gap by examining patient-specific wall stresses in autograft subregions, as well as the influence of dacron graft interposition at the STJ.

Supplementary Material

Refer to Web version on PubMed Central for supplementary material.

Sources of Funding

This study was funded by American Heart Association Postdoctoral Fellowship 16POST31420013 (Xuan), UCSF PROF-PATH/Summer Excellence Research Fellowship (Alonso), and National Institutes of Health, R01HL119857-01A1 (Tseng and Ge).

Glossary of Abbreviations

3D	3 dimensional
DICOM	Digital Imaging and Communications in Medicine
MAP	mean arterial pressure
MRI	magnetic resonance imaging
MHI	Montreal Heart Institute
UCSF	University of California San Francisco
SFVAMC	San Francisco Veterans Affairs Medical Center
FE	finite element
FEA	finite element analyses

SOV	sinuses of Valsalva
STJ	sinotubular junction
AscAo	ascending aorta
cm	centimeter
kPa	kilopascal

References

1. Laudito A, Brook MM, Suleman S, Bleiweis MS, Thompson LD, Hanley FL and Reddy VM. The Ross procedure in children and young adults: a word of caution. J Thorac Cardiovasc Surg. 2001;122:147–153. [PubMed: 11436048]
2. Kouchoukos NT, Masetti P, Nickerson NJ, Castner CF, Shannon WD and Davila-Roman VG. The Ross procedure: long-term clinical and echocardiographic follow-up. Ann Thorac Surg. 2004;78:773–81; discussion 773-81. [PubMed: 15336990]
3. Mastrobuoni S, de Kerchove L, Solari S, Astarci P, Poncelet A, Noirhomme P, Rubay J and El Khoury G. The Ross procedure in young adults: over 20 years of experience in our Institution. Eur J Cardiothorac Surg. 2015;49:507–513. [PubMed: 25736279]
4. Sievers HH, Stierle U, Charitos EI, Takkenberg JJ, Horer J, Lange R, Franke U, Albert M, Gorski A, Leyh RG, Riso A, Sachweh J, Moritz A, Hetzer R and Hemmer W. A multicentre evaluation of the autograft procedure for young patients undergoing aortic valve replacement: update on the German Ross Registrydagger. Eur J Cardiothorac Surg. 2016;49:212–8. [PubMed: 25666469]
5. El-Hamamsy I, Eryigit Z, Stevens LM, Sarang Z, George R, Clark L, Melina G, Takkenberg JJ and Yacoub MH. Long-term outcomes after autograft versus homograft aortic root replacement in adults with aortic valve disease: a randomised controlled trial. Lancet. 2010;376:524–31. [PubMed: 20684981]
6. Pettersson GB, Subramanian S, Flynn M, Nowicki ER, Batizy LH, Svensson LG and Blackstone EH. Reoperations after the ross procedure in adults: towards autograft-sparing/Ross reversal. J Heart Valve Dis. 2011;20:425–32. [PubMed: 21863656]
7. Stulak JM, Burkhart HM, Sundt TM 3rd, Connolly HM, Suri RM, Schaff HV and Dearani JA. Spectrum and outcome of reoperations after the Ross procedure. Circulation. 2010;122:1153–8. [PubMed: 20823390]
8. Schmidtke C, Bechtel J, Hueppe M, Noetzold A and Sievers HH. Size and distensibility of the aortic root and aortic valve function after different techniques of the ross procedure. J Thorac Cardiovasc Surg. 2000;119:990–7. [PubMed: 10788820]
9. Yacoub MH, El-Hamamsy I, Sievers HH, Carabello BA, Bonow RO, Stelzer P, da Costa FDA, Schafers HJ, Skillington P, Charitos EI, Luciani GB and Takkenberg JJM. Under-use of the Ross operation--a lost opportunity. Lancet. 2014;384:559–560. [PubMed: 25131967]
10. Stelzer P, Itagaki S, Varghese R and Chikwe J. Operative mortality and morbidity after the Ross procedure: a 26- year learning curve. J Heart Valve Dis. 2013;22:767–75. [PubMed: 24597396]
11. Skillington PD, Mokhles MM, Takkenberg JJ, O'Keefe M, Grigg L, Wilson W, Larobina M and Tatoulis J. Twenty-year analysis of autologous support of the pulmonary autograft in the Ross procedure. Ann Thorac Surg. 2013;96:823–9. [PubMed: 23870828]
12. Charitos EI, Stierle U, Hanke T, Bechtel M, Sievers HH and Petersen M. Pulmonary homograft morphology after the Ross procedure: a computed tomography study. J Heart Valve Dis. 2011;20:688–94. [PubMed: 22655500]
13. Luciani GB, Casali G, Favaro A, Prioli MA, Barozzi L, Santini F and Mazzucco A. Fate of the aortic root late after Ross operation. Circulation. 2003;108:II-61–II-67. [PubMed: 12970210]
14. Mokhles MM, Rizopoulos D, Andrinopoulou ER, Bekkers JA, Roos-Hesselink JW, Lesaffre E, Bogers AJJC and Takkenberg JJM. Autograft and pulmonary allograft performance in the second

post-operative decade after the Ross procedure: insights from the Rotterdam Prospective Cohort Study. European heart journal. 2012;33:2213–2224. [PubMed: 22730489]

15. Charitos EI, Stierle U, Hanke T, Schmidtke C, Sievers HH and Richardt D. Long-term results of 203 young and middle-aged patients with more than 10 years of follow-up after the original subcoronary Ross operation. Ann Thorac Surg. 2012;93:495–502. [PubMed: 22197618]
16. Sievers H, Dahmen G, Graf B, Stierle U, Ziegler A and Schmidtke C. Midterm results of the Ross procedure preserving the patient's aortic root. Circulation. 2003;108 Suppl 1:II55–60. [PubMed: 12970209]
17. Forcillo J, Cikirikcioglu M, Poirier N and El-Hamamsy I. The Ross procedure: total root technique. Multimed Man Cardiothorac Surg. 2014;2014.
18. Stelzer P, Weinrauch S and Tranbaugh RF. Ten years of experience with the modified Ross procedure. J Thorac Cardiovasc Surg. 1998;115:1091–100. [PubMed: 9605079]
19. Charitos EI, Hanke T, Stierle U, Robinson DR, Bogers AJ, Hemmer W, Bechtel M, Misfeld M, Gorski A, Boehm JO, Rein JG, Botha CA, Lange R, Hoerer J, Moritz A, Wahlers T, Franke UF, Breuer M, Ferrari-Kuehne K, Hetzer R, Huebler M, Ziemer G, Takkenberg JJ and Sievers HH. Autograft reinforcement to preserve autograft function after the ross procedure: a report from the german-dutch ross registry. Circulation. 2009;120:S146–54. [PubMed: 19752360]
20. Carrel T The autograft inclusion: an obligatory step to avoid late failure following the Ross procedure? J Thorac Cardiovasc Surg. 2015;149:S53–4. [PubMed: 25304304]
21. Wisneski AD, Matthews PB, Azadani AN, Mookhoek A, Chitsaz S, Guccione JM, Ge L and Tseng EE. Human pulmonary autograft wall stress at systemic pressures prior to remodeling after the Ross procedure. J Heart Valve Dis. 2014;23:377–84. [PubMed: 25296465]
22. Mookhoek A, Krishnan K, Chitsaz S, Kuang H, Ge L, Schoof PH, Bogers AJ, Takkenberg JJ and Tseng EE. Biomechanics of Failed Pulmonary Autografts Compared With Normal Pulmonary Roots. Ann Thorac Surg. 2016;102:1996–2002. [PubMed: 27457832]
23. Dionne PO, Wener E, Emmott A, Cartier R, Mongrain R, Leask R and El-Hamamsy I. The Ross procedure: biomechanical properties of the pulmonary artery according to aortic valve phenotype. Interact Cardiovasc Thorac Surg. 2016;23:371–6. [PubMed: 27241051]
24. Xuan Y, Wang Z, Liu R, Haraldsson H, Hope MD, Saloner DA, Guccione JM, Ge L and Tseng E. Wall stress on ascending thoracic aortic aneurysms with bicuspid compared with tricuspid aortic valve. J Thorac Cardiovasc Surg. 2018;156:492–500. [PubMed: 29656820]
25. Speelman L, Bosboom EM, Schurink GW, Hellenthal FA, Buth J, Breeuwer M, Jacobs MJ and van de Vosse FN. Patient-specific AAA wall stress analysis: 99-percentile versus peak stress. Eur J Vasc Endovasc Surg. 2008;36:668–76. [PubMed: 18851924]
26. Xuan Y DD, Wisneski A, Wang Z, Ye J, Guccione J, Ge L, Tseng E. Impact of Transcatheter Aortic Valve Size on Leaflet Stresses: Implications for Durability and Optimal Grey Zone Sizing. AsiaIntervention. 2020;In press.
27. Hokken RB, Bogers AJJC, Taams MA, Schiks-Berghourt MB, Herwerden LAv, Roelandt JRTC and Bos E. Does the pulmonary autograft in the aortic position in adults increase in diameter? An echocardiographic study. J Thorac Cardiovasc Surg. 1997;113:667–674. [PubMed: 9104975]
28. Carr-White GS, Kilner PJ, Hon JK, Rutledge T, Edwards S, Burman ED, Pennell DJ and Yacoub MH. Incidence, location, pathology, and significance of pulmonary homograft stenosis after the Ross operation. Circulation. 2001;104:I16–20. [PubMed: 11568023]
29. David TE, Omran A, Ivanov J, Armstrong S, de Sa MP, Sonnenberg B and Webb G. Dilation of the pulmonary autograft after the Ross procedure. J Thorac Cardiovasc Surg. 2000;119:210–20. [PubMed: 10649195]
30. Brown JW, Ruzmetov M, Shahriari AP, Rodefeld MD, Mahomed Y, Turrentine MW. Modification of the Ross aortic valve replacement to prevent late autograft dilatation. Eur J Cardiothorac Surg. 2010;37(5):1002–1007. [PubMed: 20138780]
31. Slater M, Shen I, Welke K, Komanapalli C, and Ungerleider R. Modification to the Ross Procedure to Prevent Autograft Dilatation. Semin Thorac Cardiovasc Pediatr Card Surg Ann. 2005;8:181–184.

32. Jacobsen RM, Earing MG, Hill GD, Barnes M, Mitchell ME, Woods RK, and Tweddell JS. The Externally Supported Ross Operation: Early Outcomes and Intermediate Follow-Up. Ann Thorac Surg. 2015;100:631–638. [PubMed: 26141776]

33. Grande KJ, Cochran RP, Reinhall PG and Kunzelman KS. Stress variations in the human aortic root and valve: the role of anatomic asymmetry. Ann Biomed Eng. 1998;26:534–45. [PubMed: 9662146]

34. Krishnan K, Ge L, Haraldsson H, Hope MD, Saloner DA, Guccione JM and Tseng EE. Ascending thoracic aortic aneurysm wall stress analysis using patient-specific finite element modeling of in vivo magnetic resonance imaging. Interact Cardiovasc Thorac Surg. 2015;21:471–80. [PubMed: 26180089]

Central Message

At one-year postoperatively, patient-specific simulations after Ross procedure revealed that all autograft regions had elevated wall stresses compared to native distal aorta without early dilatation.

Perspective Statement

Elevated wall stresses may lead to autograft dilatation requiring reoperation. Using finite element modeling of patient-specific autografts, we found wall stresses in all autograft regions were greater than distal ascending aorta without concurrent dilatation at one-year post-Ross operation. Our work provides the necessary first step towards understanding how autograft wall stresses lead to dilatation.

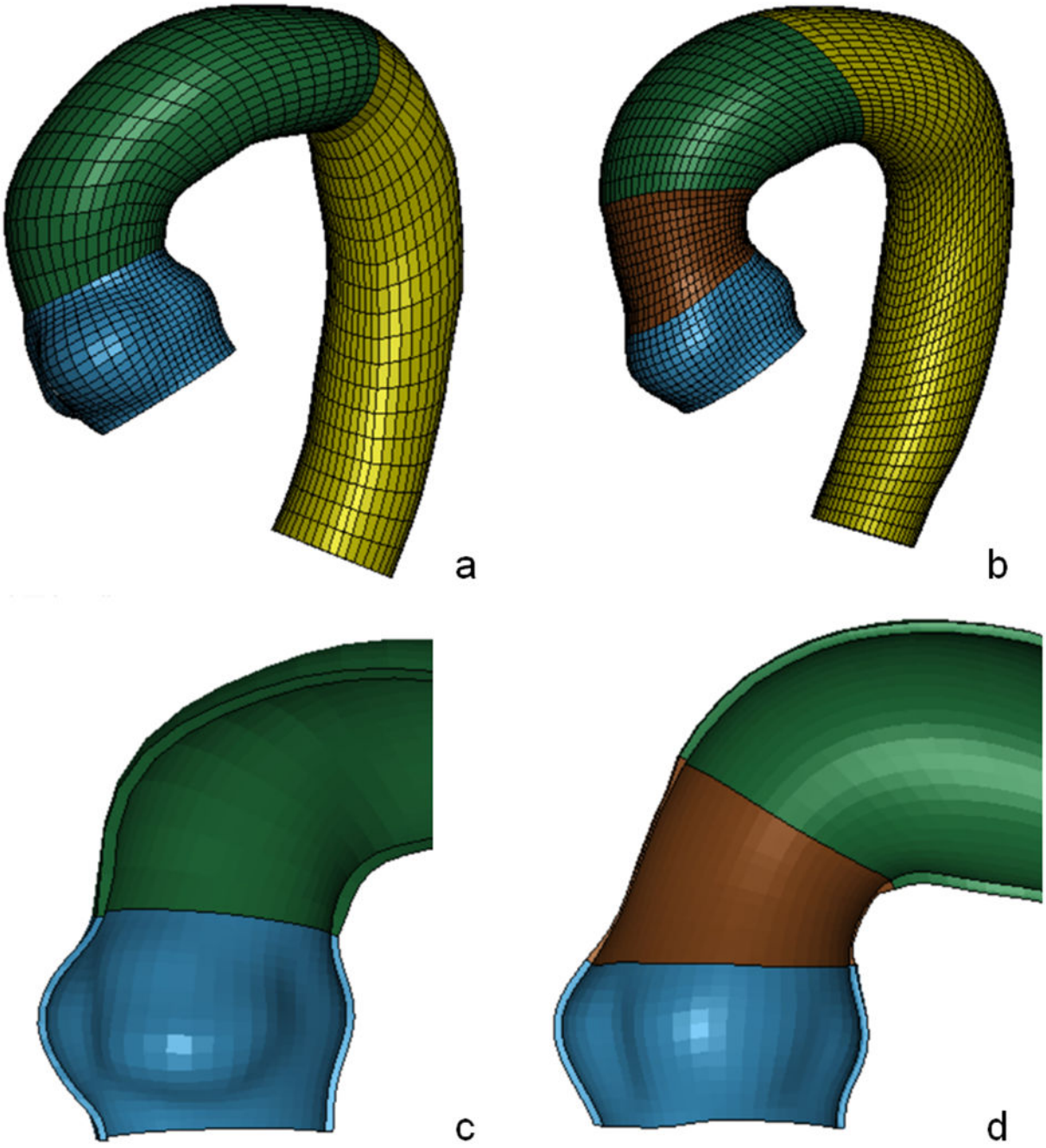

Figure 1.

Representative 3D mesh models of pulmonary autograft and ascending aorta without(a) and with Dacron interposition graft(b); cross section of autograft and ascending aorta mesh showing the thickness variation without(c) and with Dacron interposition(d).

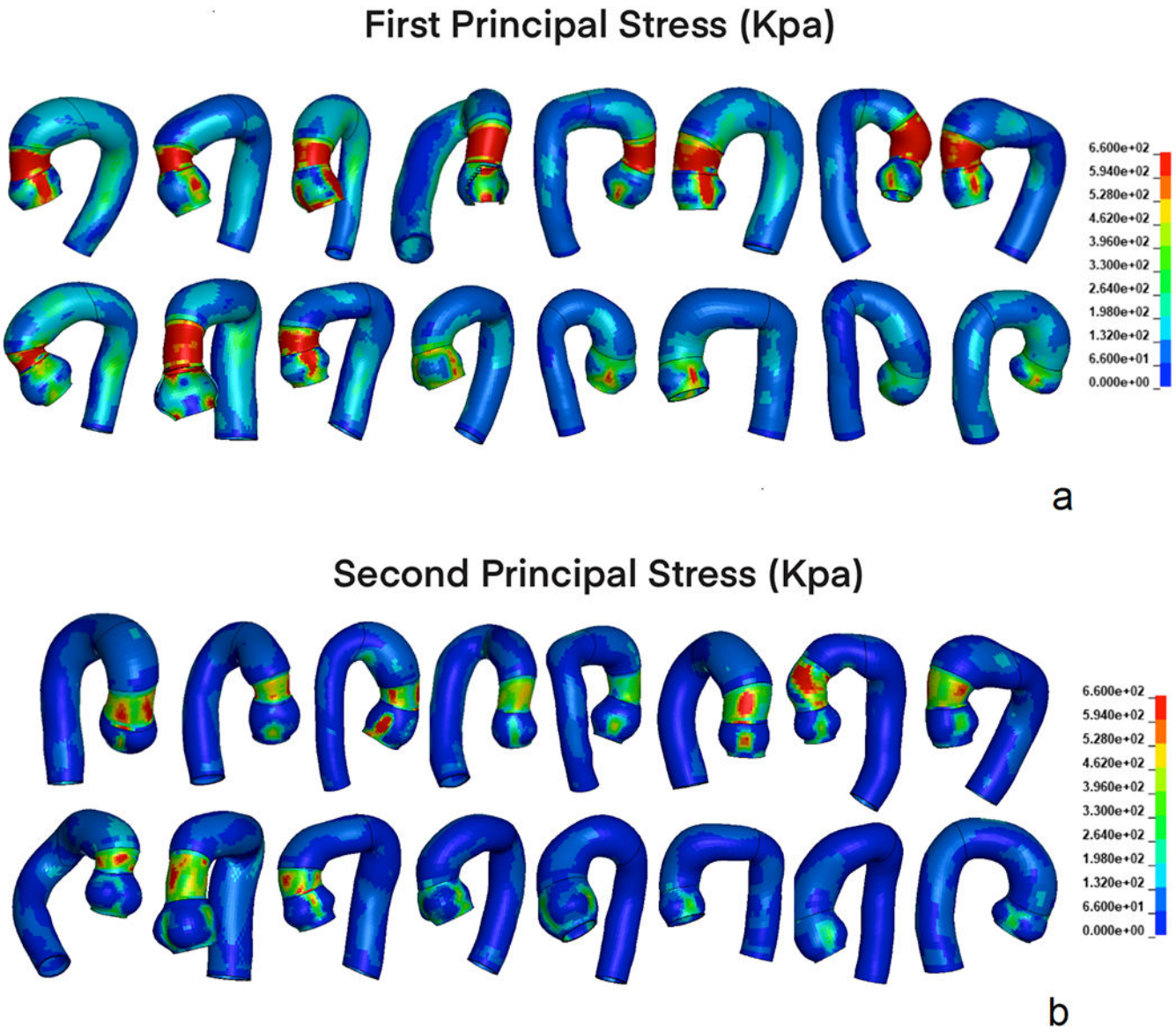

Figure 2.

a. First principal wall stress profiles (circumferential stresses) of patient-specific autograft and ascending aorta models (top) b. Second principal wall stress profiles (longitudinal stresses) of patient-specific autograft and ascending aorta models (bottom). First row and the first 3 of the second row had Dacron interposition graft to the ascending aorta and the remaining did not have Dacron graft. Each individual patient in left-to-right order in (a) is reflected in the same order in (b).

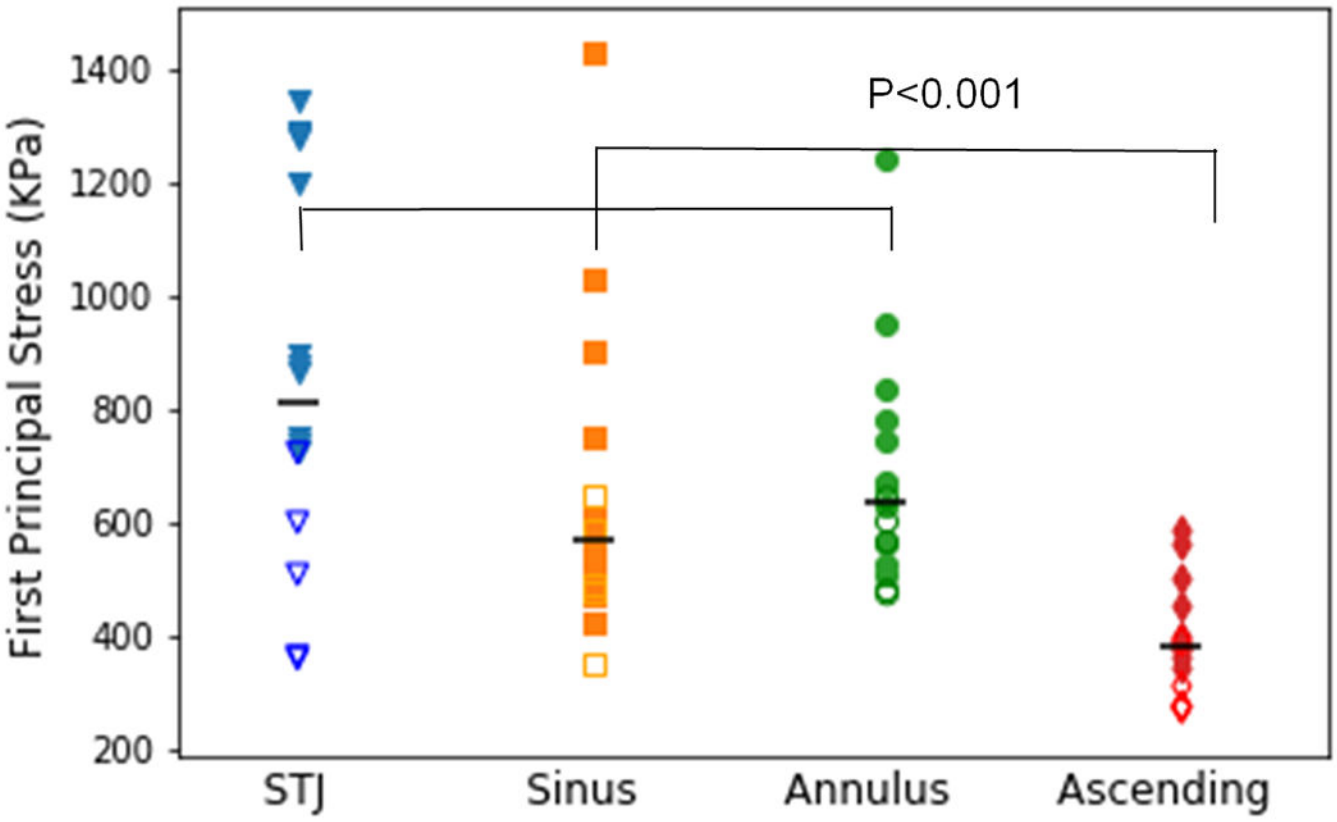

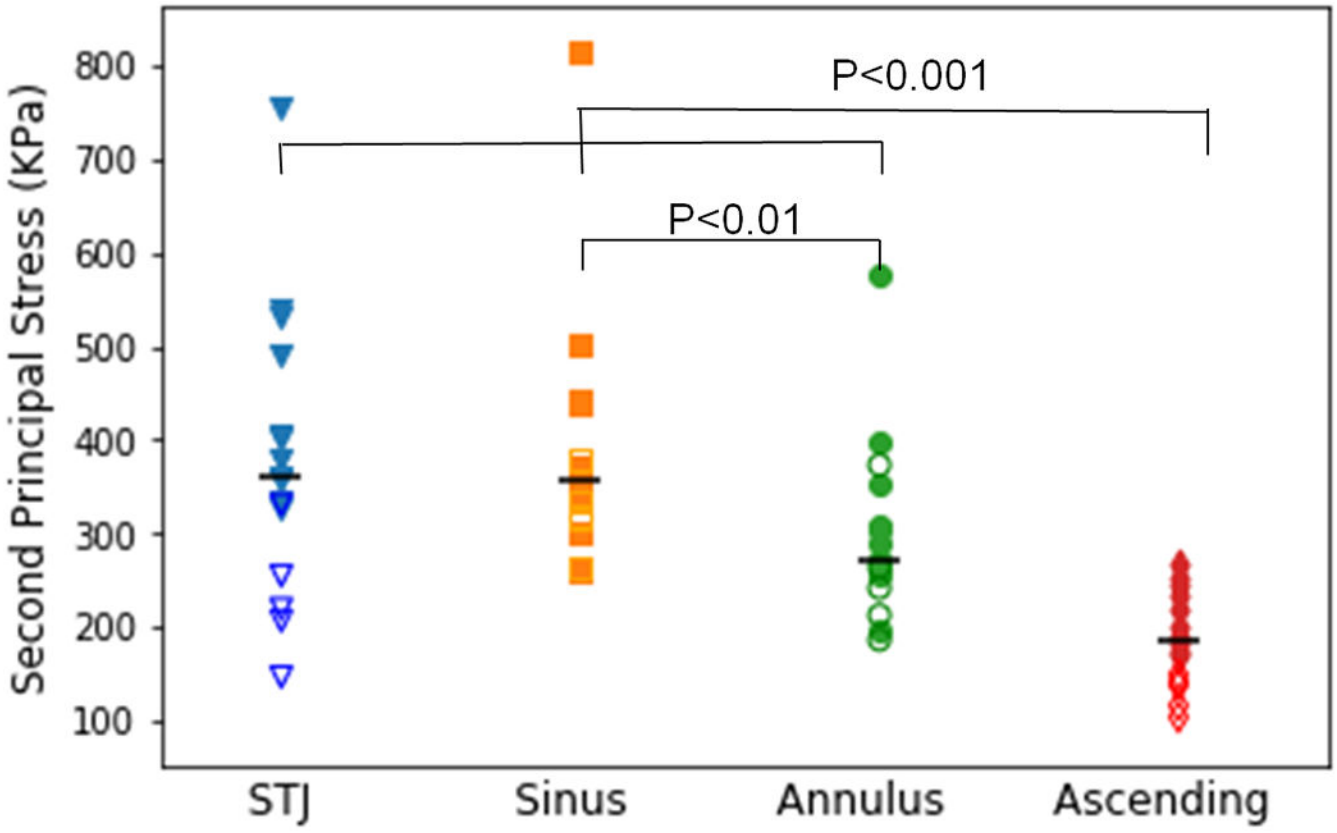

Figure 3.

Comparison of autograft subregions and ascending aorta: peak first (a) and second (b) principal wall stresses (solid markers=patients with Dacron interposition; unfilled markers=patients without Dacron interposition; black bar=median value). The first and second principal stresses on sinotubular junction, sinus, and autograft annulus were higher than ascending aorta. The second principal stresses on sinuses were larger than that in the annulus.

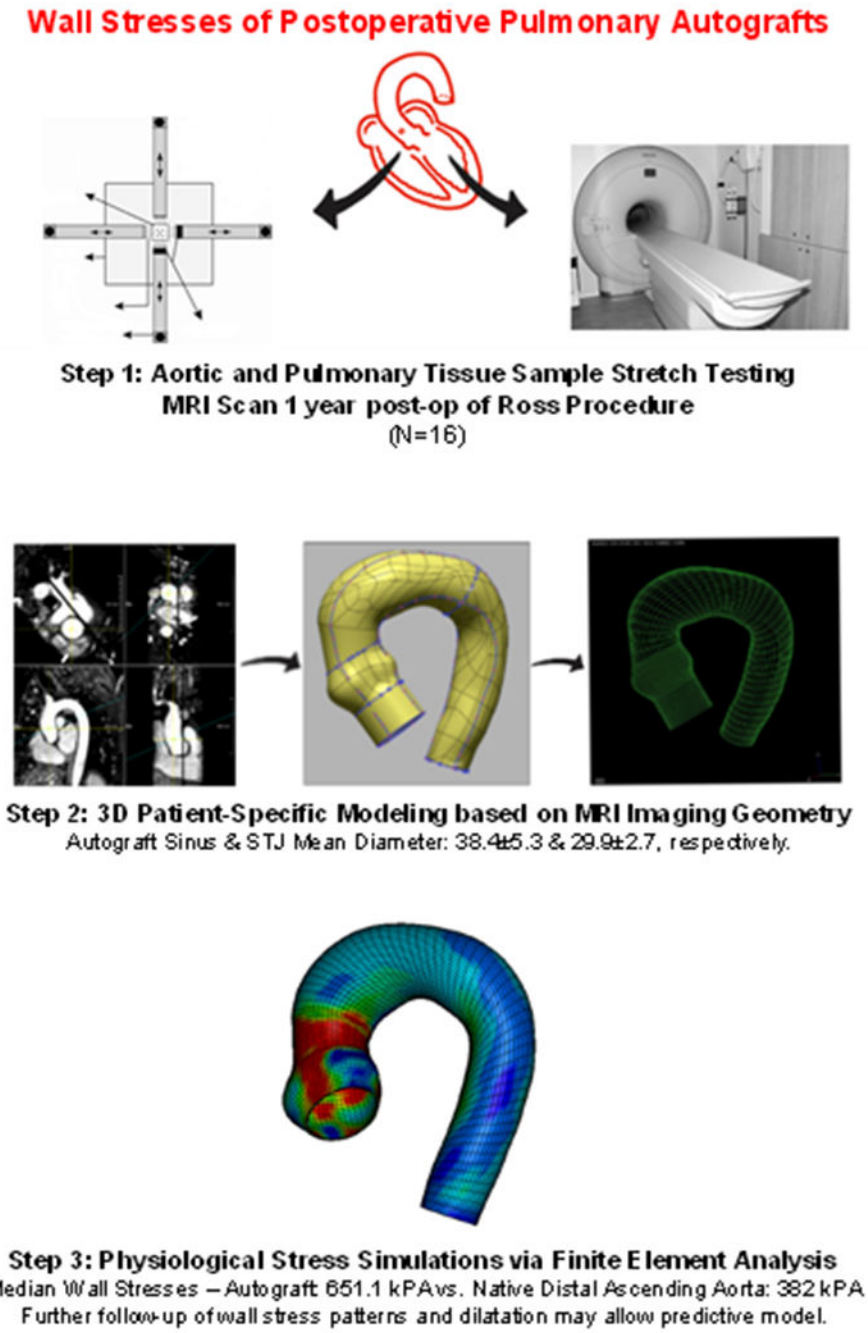

Figure 4.

Of 290 patients undergoing Ross procedure at Montreal Heart Institute, a subset of n=16 patients had autograft and aortic tissue removed during surgery for biaxial stretch testing for material properties and postoperative magnetic resonance imaging at 1 year. Patient-specific modeling of pulmonary autografts were performed using 3D patient-specific imaging and material properties. Finite element analyses were performed to determine wall stresses in the autograft and ascending aorta. Pulmonary autograft had significantly higher wall stresses than distal ascending aorta (native internal control) which could drive remodeling over time.

Future clinical follow-up can provide understanding of autograft biomechanics in relation to clinical dilatation.

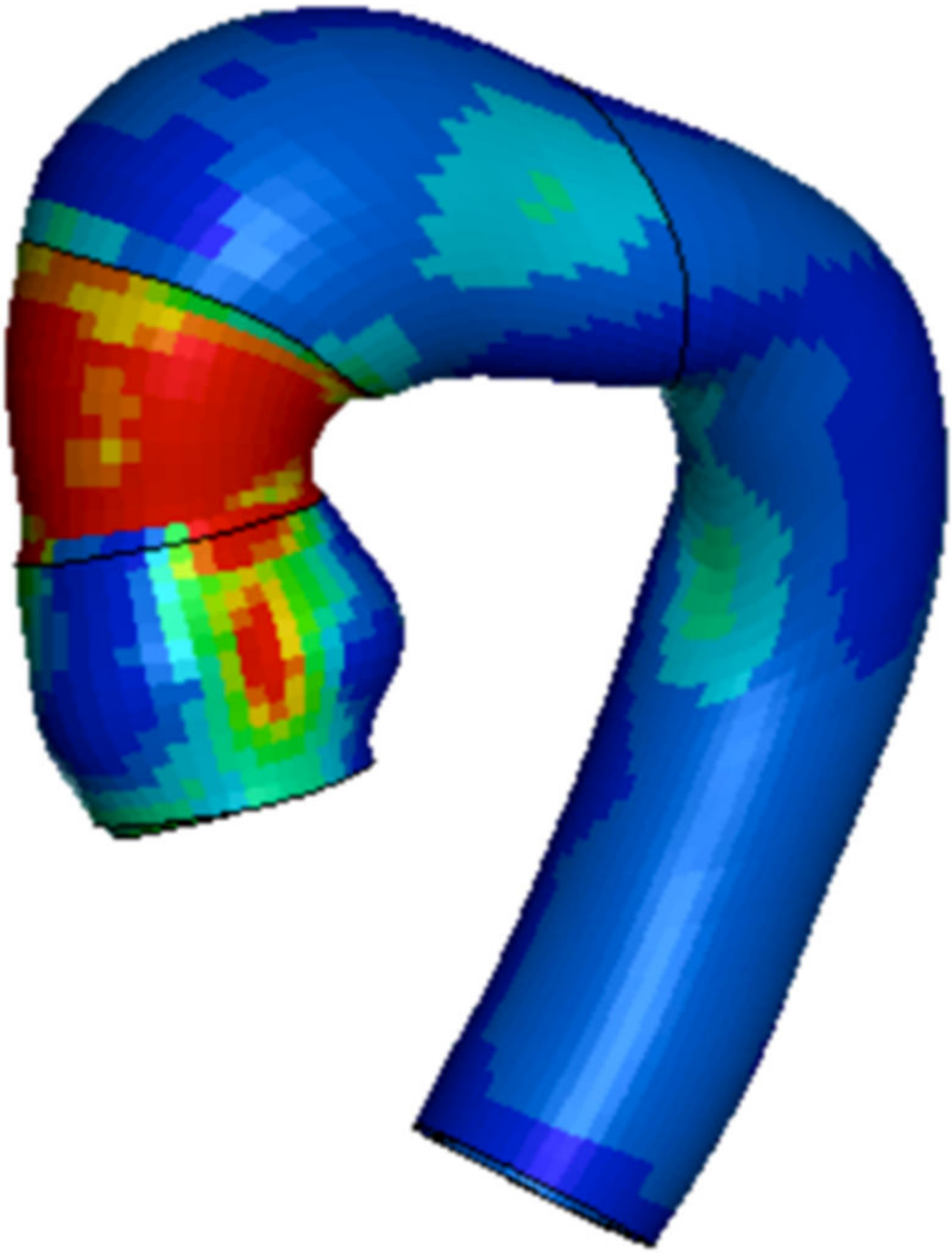

Central Figure.
First principal stresses of representative patient-specific autograft, ascending aorta, and Dacron graft.

Table 2.

Patient-specific Characteristics (N=16).

	Age	Sex	Autograft Thickness (mm)	Aortic Thickness (mm)	Dacron Graft	NYHA	Valve Morphology	Stenosis/ Regurgitation/Mixed
1	50	M	1.00	1.40	Y	3	BAV	Mixed
2	58	F	0.84	1.35	Y	2	BAV	Stenosis
3	59	F	1.36	2.05	Y	3	BAV	Stenosis
4	57	F	0.84	1.81	Y	2	BAV	Stenosis
5	56	M	1.24	1.85	Y	3	BAV	Mixed
6	50	M	1.29	2.29	Y	2	BAV	Mixed
7	23	F	0.69	1.24	Y	2	BAV	Stenosis
8	60	M	1.29	1.81	Y	2	BAV	Stenosis
9	28	F	1.16	*	N	3	UAV	Stenosis
10	53	M	1.15	*	N	3	BAV	Mixed
11	52	M	1.32	*	Y	3	BAV	Stenosis
12	17	F	1.19	*	N	2	BAV	Mixed
13	53	M	1.4	1.78	Y	2	BAV	Stenosis
14	54	M	1.48	*	N	1	UAV	Mixed
15	41	M	1.35	1.625	Y	3	UAV	Mixed
16	53	M	1.07	*	N	3	BAV	Stenosis

*Aortic Thickness was not measured, averaged value used (1.84 mm)

Table 3.

Patient-specific Pulmonary and Aortic Diameters

	Pulm. Autograft Pre-op: Max Diameter (cm)			Aorta Pre-op: Max Diameter (cm)				1yr Post-op: Max Diameter (cm)			
	Annulus	**Sinus**	**STJ**	**Annulus**	**Sinus**	**STJ**	**A.A.**	**Annulus**	**Sinus**	**STJ**	**A.A.**
1	2.4	2.7	2.5	3.4	3.7	3.0	3.5	2.9	3.8	3.2	3.7
2	2.0	2.2	2.2	2.3	2.8	2.1	3.5	2.2	3.1	2.7	3.1
3	2.3	2.4	2.8	3.2	2.9	3.0	3.6	2.3	3.3	2.8	4.0
4	2.9	2.8	2.7	3.1	3.8	3.7	4.3	2.4	3.5	2.9	3.0
5	2.8	3.0	2.8	4.6	4.6	3.7	4.2	3.0	3.8	2.9	3.7
6	2.2	2.3	2.7	3.6	3.9	4.1	4.4	2.5	3.9	2.9	3.4
7	2.3	2.3	2.6	3.1	3.8	3.5	4.1	2.8	3.4	2.9	3.3
8	*	*	*	*	*	*	*	2.2	3.9	2.8	3.5
9	2.4	2.6	2.3	2.2	2.4	2.2	2.6	1.9	3.1	2.7	3.0
10	2.2	2.4	2.5	2.9	3.6	3.0	2.7	2.8	3.5	3.0	3.6
11	3.2	3.2	3.4	4.0	4.6	4.2	4.5	2.8	4.2	3.0	3.9
12	*	*	*	*	*	*	*	2.3	3.5	3.0	3.1
13	3.1	3.0	3.0	3.8	4.3	4.0	4.2	3.0	4.4	2.9	3.6
14	4.5	3.6	3.6	4.3	4.7	3.6	3.6	3.3	4.8	3.8	4.2
15	3.9	3.9	3.8	4.3	4.3	3.5	4.1	2.8	4.8	3.0	4.2
16	3.0	3.3	3.4	3.3	4.1	3.0	3.2	3.3	4.3	3.3	3.7
Avg. ± SD	2.8 ± 0.7	2.8 ± 0.5	2.9 ± 0.5	3.4 ± 0.7	3.8 ± 0.7	3.3 ± 0.7	3.8 ± 0.6	2.7 ± 0.4	3.8 ± 0.5	3.0 ± 0.3	3.6 ± 0.4

Avg. = Average; A.A. = Ascending Aorta;

*No pre-operative imaging available

Table 4.

Peak first and second principal wall stresses in each subregion under systolic pressure, comparing patient-specific and group-averaged (Avg) material properties at 1-year post Ross procedure.

	Peak First Principal Stress			Peak Second Principal Stress		
(KPa)	**Patient-Specific Material Property**	**Avg Material Property**	**P**	**Patient-Specific Material Property**	**Avg Material Property**	**P**
Sinotubular Junction	809 (691-1219)	777(689-1225)	0.90	360 (310-426)	338(304-421)	0.70
Sinus	567 (485-675)	570(485-676)	0.98	355 (320-394)	355(320-392)	0.98
Annulus	637 (555-755)	642(527-751)	0.98	272 (252-319)	294(269-340)	0.40
Ascending Aorta	382 (334-413)	373(324-413)	0.72	184(147-222)	182(147-223)	0.95

Data presented as median (25-75% interquartile range).

Table 5.

Distensibility of the subregions of the pulmonary autograft.

%	With Dacron replacement	Without Dacron replacement	P value
Sinotubular Junction	0.03±0.01	3.38±0.69	0.001
Sinus	0.99±0.28	1.22±0.23	0.087
Annulus	3.48±0.64	4.20±0.44	0.016

Distensibility was defined as (perimeter at systole − perimeter at diastole)/ perimeter at diastole.